MOLECULAR AND CELLULAR BIOLOGY, Jan. 1993, p. 703–710
0270-7306/93/010703-08$02.00/0

Vol. 13, No. 1

The Cellular RNA-Binding Protein EAP Recognizes a Conserved Stem-Loop in the Epstein-Barr Virus Small RNA EBER 1

DAVID P. TOCZYSKI* AND JOAN A. STEITZ

Department of Molecular Biophysics and Biochemistry, Howard Hughes Medical Institute, Yale University, 295 Congress Avenue, New Haven, Connecticut 06536-0812

Received 17 August 1992/Returned for modification 1 October 1992/Accepted 23 October 1992

EAP (EBER-associated protein) is an abundant, 15-kDa cellular RNA-binding protein which associates with certain herpesvirus small RNAs. We have raised polyclonal anti-EAP antibodies against a glutathione *S*-transferase–EAP fusion protein. Analysis of the RNA precipitated by these antibodies from Epstein-Barr virus (EBV)- or herpesvirus papio (HVP)-infected cells shows that >95% of EBER 1 (EBV-encoded RNA 1) and the majority of HVP 1 (an HVP small RNA homologous to EBER 1) are associated with EAP. RNase protection experiments performed on native EBER 1 particles with affinity-purified anti-EAP antibodies demonstrate that EAP binds a stem-loop structure (stem-loop 3) of EBER 1. Since bacterially expressed glutathione *S*-transferase–EAP fusion protein binds EBER 1, we conclude that EAP binding is independent of any other cellular or viral protein. Detailed mutational analyses of stem-loop 3 suggest that EAP recognizes the majority of the nucleotides in this hairpin, interacting with both single-stranded and double-stranded regions in a sequence-specific manner. Binding studies utilizing EBER 1 deletion mutants suggest that there may also be a second, weaker EAP-binding site on stem-loop 4 of EBER 1. These data and the fact that stem-loop 3 represents the most highly conserved region between EBER 1 and HVP 1 suggest that EAP binding is a critical aspect of EBER 1 and HVP 1 function.

Epstein-Barr virus (EBV) is a B-cell lymphotrophic herpesvirus which is able to transform primary cells in vitro (for a review, see references 18 and 25). During latency, most EBV genes are transcriptionally silent (for a review, see reference 19). A striking exception, however, is the genes for two small RNAs called EBER 1 and EBER 2 (for Epstein-Barr-encoded RNA). These RNAs are each present at approximately 5×10^6 copies per cell in latently infected B-cell lines (22). Herpesvirus papio (HVP), a related virus which infects baboons, encodes a homologous pair of small RNAs. These RNAs, HVP 1 and HVP 2, are 83 and 65% identical to the EBERs and are present at approximately 5×10^6 and 5×10^5 to 10×10^5 copies per cell, respectively (15).

The EBER genes are unusual in that they are transcribed by RNA polymerase III and yet they utilize promoter elements normally associated with protein-coding (class II) genes (16). As with most RNA polymerase III transcripts, the 3′ ends of the EBERs (and those of the HVPs) are composed of a short stretch of uridine residues. The La protein, a 50-kDa phosphoprotein first identified as an autoantigen, binds this poly(U) tail on >90% of the EBER and HVP RNAs (15). We previously identified a second protein, EAP (EBER-associated protein), which also binds to these viral small RNAs (32). EAP is an abundant, 15-kDa cellular protein which appears to be the mammalian homolog of a previously identified sea urchin protein. A cDNA encoding the sea urchin protein, which was called 217, was identified in a screen for genes expressed in a developmentally specific manner (8, 12). EAP and the 217 protein are 77% identical. Unfortunately, the functions of both remain a mystery.

We have now raised anti-EAP antibodies and have used them to characterize the interaction between EAP and the EBERs. Whereas previous experiments had suggested that EAP bound both EBER 1 and EBER 2 (32), the binding studies presented here indicate that EAP's association with EBER 1 is by far the more significant. In contrast to that of many other RNA-binding proteins, EAP's ability to bind the third stem-loop of EBER 1 is reduced by many mutations in double-stranded regions, even when secondary structure is maintained. Characterization of this binding site should aid in identifying the cellular RNAs associated with EAP.

MATERIALS AND METHODS

Glutathione transferase fusion protein and antibody production. A glutathione *S*-transferase (GST)–EAP fusion vector was prepared by inserting an EAP-encoding DNA fragment containing a 5′-terminal *Bam*HI site into an expression vector (pGEX) (2) encoding 27 kDa of the GST protein with a *Bam*HI site at its 3′ end. The EAP-encoding insert contained an open reading frame with a *Bam*HI site followed by a factor X cleavage site and the entire EAP sequence, excluding the initiating methionine. A stop codon immediately after the EAP C terminus was followed by a short polylinker including a *Bam*HI and a *Sal*I site. This insert was generated by the polymerase chain reaction from an EAP cDNA template. The terminal restriction sites and factor X cleavage site were included in the deoxyoligonucleotides: 5′, CGGATCCTGATCGAGGGCAGGGCCCCCGTGAAGAA GCTGGTGGTGAAGGGCGGAAAGAAGAAGAAGCA, and 3′, GGGATCCAGCTGTCGACTTAATCCTCGTCTT CCTCCTCTTCTTCGTCCTGG. The polymerase chain reaction was carried out as described by Toczyski and Steitz (32). The EAP insert was cloned into pGEX-3X after digestion of both the insert and the vector with *Bam*HI. The entire EAP insert was sequenced. T7 transcription, molecular cloning, bacterial techniques, DNA sequencing, and tissue

* Corresponding author.

culture were carried out as described by Toczyski and Steitz (32).

The GST-EAP fusion protein was isolated by inoculating 12 1-liter flasks of Luria broth containing 200 μg of carbenicillin with 2 ml from a fresh overnight culture of *Escherichia coli* (DH 1) transformed with the fusion protein-bearing or wild-type GST plasmid. The cells were grown to an optical density at 590 nm of 0.75 to 0.90. IPTG (isopropyl-β-D-thiogalactopyranoside) was then added to 0.05 mM, and the cells were grown for another 2 to 3 h. Cells were harvested, sonicated in Tris-buffered saline (150 mM NaCl, 50 mM Tris [pH 7.5]) containing 1% Triton X-100 six times for 30 s on a Branson Sonifier at setting 7, and centrifuged for 15 min at 15 krpm in a Sorvall SA600 rotor. At this point, the cell sonicate could be frozen after the addition of glycerol to 10%. The extract was then run over a 3- to 4-ml glutathione agarose (S linkage, Sigma) column and washed with 300 ml of Tris-buffered saline containing 1% Triton X-100. After being washed with 50 ml of 50 mM Tris, pH 8.0, the column was eluted with the same buffer containing 10 mM glutathione. A portion of this material was then boiled in 0.1% sodium dodecyl sulfate (SDS) for 5 min and used to raise antibodies in rabbits; antibodies were produced by the Berkeley Antibody Company.

Affinity purification and Western blotting (immunoblotting). The polymerase chain reaction EAP-encoding fragment mentioned above was cut with *Bam*HI and *Sal*I and cloned into pUR-292, an expression vector containing the entire β-galactosidase gene with a polylinker at the carboxy terminus (29). This protein was overexpressed and purified according to the method described in reference 13. Approximately 50 mg of the β-galactosidase–EAP fusion was dialyzed against 0.1 M borate–0.75 M NaCl–3 mM β-mercaptoethanol (pH 8.3) and incubated with 7 ml of CNBr-activated Sepharose (Pharmacia; prewashed according to the manufacturer's specifications) for 12 h at 4°C. The resin was then blocked with Tris and washed as directed by Pharmacia. A 75-ml volume of anti-EAP serum was diluted threefold with 10 mM Tris, pH 7.5, and adsorbed onto a column containing the Sepharose-linked β-galactosidase fusion protein. After the column was washed sequentially with 100 ml of 10 mM Tris (pH 7.5), 500 ml of 500 mM NaCl–10 mM Tris (pH 7.5), and 10 ml of water, antibody was eluted with 100 mM ethanolamine, pH 11.5. Approximately 1.0-ml fractions were collected into tubes containing 0.2 ml of 1.0 M Tris, pH 7.0. Peak fractions were pooled, dialyzed against PBS with 0.02% azide, and frozen in aliquots.

Protein gels were run according to the method of Ausubel et al. (2) and blotted onto nitrocellulose (Schleicher and Schuell) in 25 mM Tris–192 mM glycine–0.1% SDS–25% methanol. Membranes were then rinsed in water and allowed to dry. Blocking was performed in rinse buffer (RB) (10 mM Tris, 150 mM NaCl, 1 mM EDTA, 0.1% Triton X-100 [pH 8.0]) with 3% Carnation nonfat dry milk for at least 2 h at 25°C. Affinity-purified anti-EAP antibodies were added at a dilution of 1:5,000, and the mixture was incubated for at least 2 h at 25°C. This solution was removed, and after a 30-min wash in RB the membrane was incubated with blocking solution and a horseradish peroxidase-linked secondary antibody (Sigma) for at least 1 h at 25°C. The blot was then washed three times for 30 min in RB supplemented with 1 M NaCl. Blots were visualized with a chemiluminescent reagent according to the manufacturer's specifications (Amersham).

The titers of anti-EAP antibodies were determined by immunoprecipitating sonicate from 2×10^5 Raji cells with varying amounts of antibody and determining, by Northern (RNA) blot analysis, how much antibody was required to deplete EBER 1. Two microliters of affinity-purified serum or 10 μl of whole serum was required for such a depletion. At least a twofold excess of serum was used unless otherwise noted.

Immunoprecipitation, Northern blotting, RNA affinity selection, and RNase protection assays. Twelve-hour $^{32}PO_4$ in vivo labelling and immunoprecipitation were performed as described in reference 22. Urea polyacrylamide gels were Northern blotted onto Zeta-probe nylon membranes and probed with full-length antisense RNAs as specified by the supplier (Bio-Rad).

3′-end labelling of RNA for affinity selection was carried out by using ^{32}pCp and RNA ligase (10). Fifty microliters of bacterial sonicate (see "Affinity purification and Western blotting [immunoblotting]") was incubated with 20 mg of glutathione agarose in 1 ml of TBS (50 mM Tris, 150 mM NaCl [pH 7.5]). The resin was then washed 10 times with 15 ml of TBS–1% Triton X-100 and incubated with pCp-labelled RNA from 10^5 Raji cells. After a 15-min incubation at 25°C, the mixture was washed seven times with NET-2 (50 mM Tris, 150 mM NaCl, 0.05% Nonidet P-40 [pH 7.5]) at 4°C. RNA was then extracted with phenol-chloroform-isoamyl alcohol (25:25:1), ethanol precipitated, and electrophoresed on a urea polyacrylamide gel.

For RNase protection experiments, sonicate from 10^6 cells was incubated with 50 μl of whole anti-EAP serum bound to 5 μg of protein A-Sepharose. After 90 min at 4°C, samples were washed five times with 1 ml of NET-2 and once with NET (NET-2 without Nonidet P-40). Samples were adjusted to 250 μl with NET containing 1,250 U of RNase T_1 (Calbiochem). After being incubated at 30°C, samples were washed four times with cold NET-2 and incubated with NET-2 containing 0.5% SDS–0.5 mg of proteinase K per ml for 15 min at 30°C. Samples were extracted with phenol-chloroform-isoamyl alcohol and ethanol precipitated. One-fourth of this sample was then 5′ end labelled with polynucleotide kinase and [γ-^{32}P]ATP. After being electrophoresed on a 15% polyacrylamide gel, bound fragments were sequenced with a Pharmacia RNA-sequencing kit.

In vitro production of EBER variants and analysis of EAP binding. An EBER 1 gene was constructed so that after cleavage with *Dra*I, transcription by T7 RNA polymerase yielded an RNA identical to EBER 1 except that the initiating A residue was replaced by GGGCG. For EB1ΔSTLP, the nucleotides between and including C60 and G83 of EBER 1 were deleted. The HSUR 3 construct was kindly supplied by Vic Myer (26). Wild-type and mutant stem-loop 3 RNAs were transcribed from overlapping deoxyoligonucleotides which were end filled under polymerase chain reaction conditions (32). In each case, one deoxyoligonucleotide represented the template preceded by the T7 RNA polymerase promoter sequence and a second deoxyoligonucleotide contained the complement of the T7 promoter followed by a short polylinker.

In the competition experiment (see Fig. 5), RNAs (regardless of length) were internally labelled to a specific activity of 0.33 μCi/pmol with [α-^{32}P]GTP. An 80-μl volume of BJAB whole-cell sonicate, prepared as for immunoprecipitation, from 8×10^5 cells was mixed with 10 μg of yeast total RNA (as a nonspecific competitor), 40 U of RNasin (Boehringer Mannheim), a specified amount of unlabeled, in vitro-transcribed EBER 1, and 400 cpm of the test RNA (≈0.8 fmol). This mixture was brought to 100 μl with water and incubated at 25°C for 10 to 15 min. The reaction mixtures were then

immunoprecipitated with anti-EAP serum. Testing of mutant hairpins (see Fig. 7) was carried out in a similar fashion, with the following exceptions. RNAs were transcribed with [α-^{32}P]CTP to a specific activity of 0.67 μCi/pmol, 600 cpm (≈0.6 fmol) of each RNA was added to the sonicate from 5 × 10^5 BJAB cells, and no unlabelled EBER 1 was added.

Quantitations were performed with a Molecular Dynamics phosphoimager. Precipitation of mutant stem-loop RNAs was corrected for loading and loss of sample by multiplying each percent precipitated value (the amount in the pellet lane divided by the combined amount in the pellet and supernatant lanes) by the ratio of the percent precipitation of the internal control (EBER 1) for that lane to the average percent precipitation for the internal control.

RESULTS

Production and characterization of anti-EAP antibodies. The human EAP polypeptide contains 128 amino acids, with the first amino acid (methionine) being removed posttranslationally (32). We constructed an expression vector encoding an EAP fusion protein that contains amino acids 2 to 128 of EAP (15 kDa) downstream of GST (27 kDa). *E. coli* expressing this EAP fusion protein grew more poorly than those strains expressing GST alone. Uninduced colonies of *E. coli* containing the GST-EAP fusion construct were smaller, and growth in liquid culture immediately ceased upon induction of GST-EAP but not upon induction of GST alone. Although the fusion protein (42 kDa) was produced at a lower level than the transferase alone (Fig. 1a; compare lanes 2 and 5), it was easily purified on glutathione agarose (lane 6).

The GST-EAP fusion protein was denatured by boiling in 0.1% SDS and was used to generate antibodies in rabbits. The rabbit antiserum was affinity purified on a β-galactosidase–EAP fusion protein column (see Materials and Methods) to select anti-EAP from anti-GST antibodies. Western blot analyses (Fig. 1b) of total protein from Raji cells (a human B-cell tissue culture line carrying EBV) showed a specific band of 15 kDa which is detected by both the crude immune and the affinity-purified anti-EAP antibodies (lanes 2 and 4, respectively) but not by the preimmune serum or the affinity effluent (lanes 1 and 3, respectively).

Using the bacterially expressed GST-EAP fusion protein allowed us to establish that the previously characterized interaction between EAP and EBER 1 (32) represents a direct association which is independent of other cellular and viral proteins. Total RNA from Raji cells was end labeled with ^{32}pCp and T4 RNA ligase. The RNA was then incubated with GST-EAP fusion protein which had been immobilized on glutathione agarose beads. Figure 2a shows that such a procedure quantitatively selects EBER 1 (lane 3). EBER 2, which indirect experiments had previously suggested is also bound by EAP (32), remains in the supernatant (lane 2). Similar experiments utilizing the wild-type GST protein did not show significant precipitation of any RNA (data not shown).

To identify other RNA species that bind EAP, we examined the RNA in native EAP particles by performing immunoprecipitation with affinity-purified anti-EAP antibodies on whole-cell extract prepared from tissue culture cells labelled with $^{32}PO_4$ in vivo. The precipitation profile obtained from BJAB cells (an uninfected B-lymphocyte cell line) shows above-background levels of several RNAs, including 5S and 5.8S rRNAs (Fig. 2b; compare lanes 7 and 4). Nearly equivalent levels of these RNAs appear in immunoprecipi-

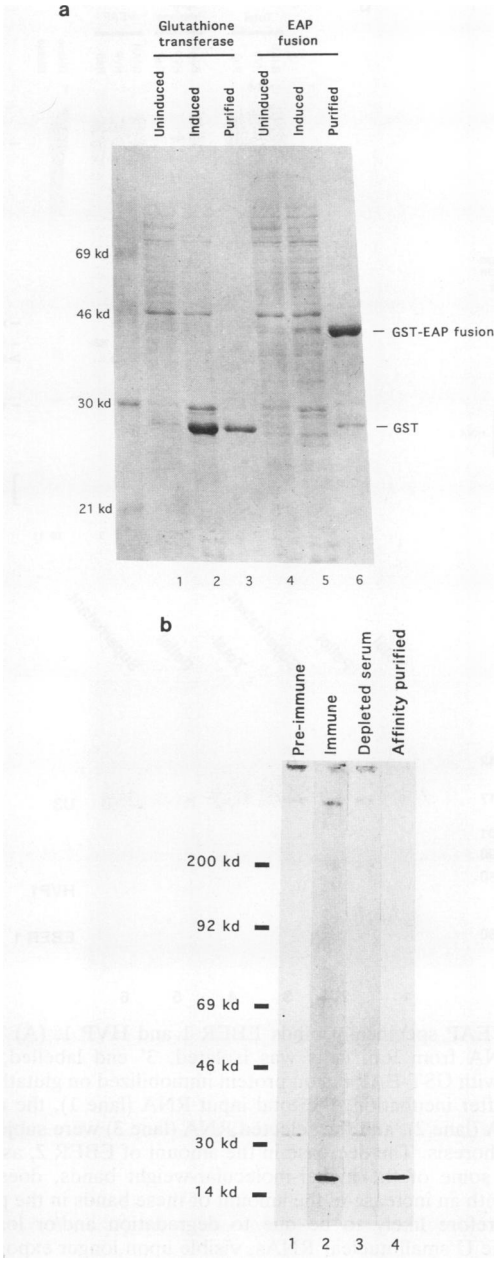

FIG. 1. Characterization of antibodies raised against a GST-EAP fusion protein. (A) Total protein from either uninduced or induced *E. coli* containing an expression vector encoding GST or a GST-EAP fusion (as indicated at the top) was fractionated on an SDS–10% polyacrylamide gel and stained with Coomassie blue. Lanes 3 and 6 contain affinity-purified GST and GST-EAP fusion protein, respectively. (B) Total cell sonicate from 2 × 10^4 Raji cells was fractionated on a 13% polyacrylamide gel and Western blotted. Four identical blots were probed with equivalent amounts of rabbit preimmune serum (lane 1), immune serum (lane 2), effluent from the affinity purification (lane 3), or the affinity-purified antibodies (lane 4). Molecular size markers (in kilodaltons) for both panels are on the left.

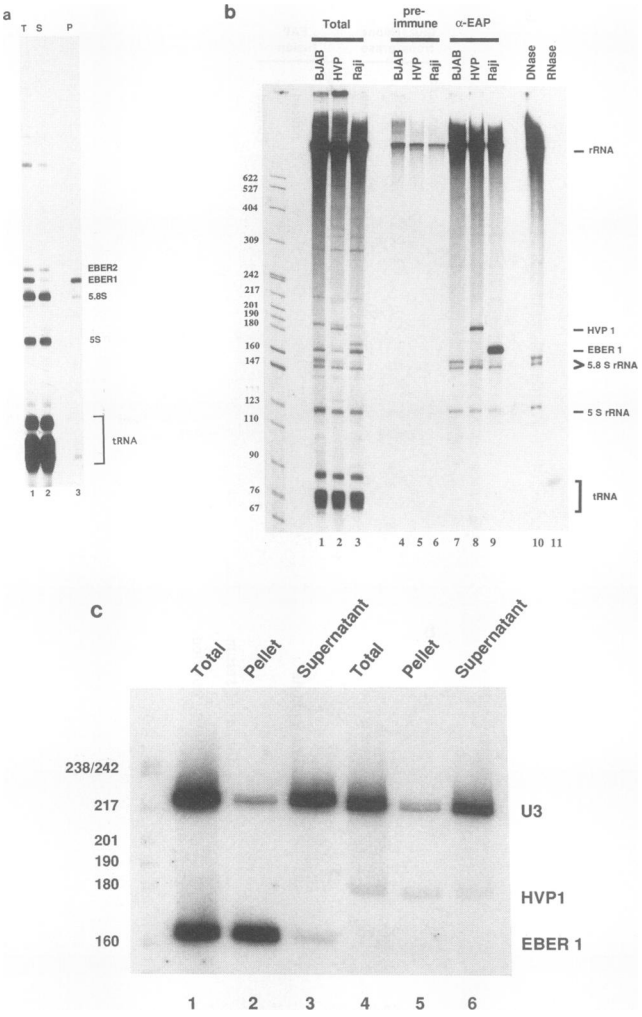

FIG. 2. EAP specifically binds EBER 1 and HVP 1. (A) Total cellular RNA from Raji cells was isolated, 3′ end labelled, and incubated with GST-EAP fusion protein immobilized on glutathione agarose. After incubation, the total input RNA (lane 1), the unselected RNA (lane 2), and the selected RNA (lane 3) were subjected to electrophoresis. The decrease in the amount of EBER 2, as well as that in some of the higher-molecular-weight bands, does not correlate with an increase in the amount of these bands in the pellet and is therefore likely to be due to degradation and/or loss of sample. The U small nuclear RNAs, visible upon longer exposures of the gel, are not selected in these experiments. (B) Uninfected B lymphocytes (BJAB) and lymphocytes infected with EBV (Raji cells) or HVP were in vivo labelled with $^{32}PO_4$. The labelled cell sonicate was immunoprecipitated with preimmune serum (lanes 4 to 6) or affinity-purified anti-EAP antibodies (lanes 7 to 9). BJAB RNA precipitated with anti-EAP serum (as in lane 7) was treated with either DNase I (lane 10) or RNase A (lane 11). One-fifteenth of the total cell sonicates were loaded in lanes 1 to 3. (C) Total RNA, RNA precipitated by affinity-purified anti-EAP antibodies, or RNA from the immunoprecipitation supernatants from either Raji cell (lanes 1 to 3) or HVP cell (lanes 4 to 6) extracts was electrophoresed and Northern blotted. The blot was probed with EBER 1 and U3 antisense RNAs. All samples were fractionated on 8.3 M urea–5% polyacrylamide sequencing gels.

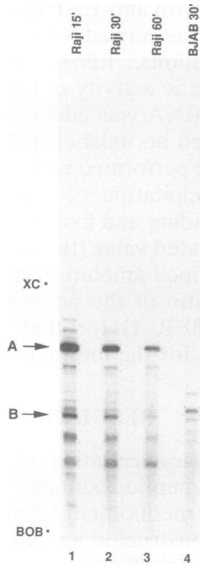

FIG. 3. RNase protection analysis of the EAP-binding site. Anti-EAP immunoprecipitates from BJAB or Raji cell sonicates were incubated with RNase T_1 for 15 (15′), 30 (30′), or 60 (60′) min. After being incubated, the precipitates were washed, deproteinized, 5′ end labelled, and subjected to electrophoresis on a 15% polyacrylamide gel. The primary RNase protection fragments are labeled A and B. The locations of the xylene cyanol (XC) and bromophenol blue (BOB) dyes are indicated.

tates from cells infected with HVP or EBV (Raji) (lanes 8 and 9, respectively), which also show strong precipitation of HVP 1 or EBER 1. To investigate the nature of the high-molecular-weight material in these profiles, aliquots of BJAB RNA precipitated with anti-EAP serum (equivalent to that in Fig. 2b, lane 7) were treated with either DNase (lane 10) or RNase (lane 11). The digestion of this material with RNase, but not with DNase, suggests that it is high-molecular-weight RNA (probably 18S and/or 28S rRNA). We therefore conclude that no cellular small RNAs, with the possible exception of rRNAs, are detectably associated with EAP.

To determine what percentage of EBER 1 or HVP 1 is associated with EAP, a Northern blot of RNA immunoprecipitated from extracts of cells infected with EBV (Fig. 2c, lanes 1 to 3) or HVP (lanes 4 to 6) was hybridized with a probe specific for EBER 1. Note that Northern blot analysis was essential since EBER 1 comigrates with U1 small nuclear RNA. The results indicate that at least 50 to 60% of HVP 1 (lane 5 compared with lane 4) and >95% of EBER 1 (lane 2 compared with lane 1) are associated with EAP. Since an antisense EBER 1 probe was used, HVP 1 (which is only 83% similar to EBER 1) is underrepresented in the autoradiograph. This blot was simultaneously probed for the U3 small nuclear RNA to control for nonspecific immunoprecipitation (≤10%).

EAP binds the third stem-loop of EBER 1. RNase protection analyses were performed to determine which portion(s) of EBER 1 is recognized by EAP. Anti-EAP immunoprecipitates from Raji (EBV-infected) or BJAB (uninfected) cells were treated with limiting amounts of RNase T_1 for various times, washed, and 5′ end labelled with polynucleotide kinase. One major and one minor band (labeled A and B in Fig. 3, lanes 1 to 3) appeared consistently with immune serum. The other immunoprecipitated fragments seen in Fig. 3 are much less likely to represent important EAP-RNA

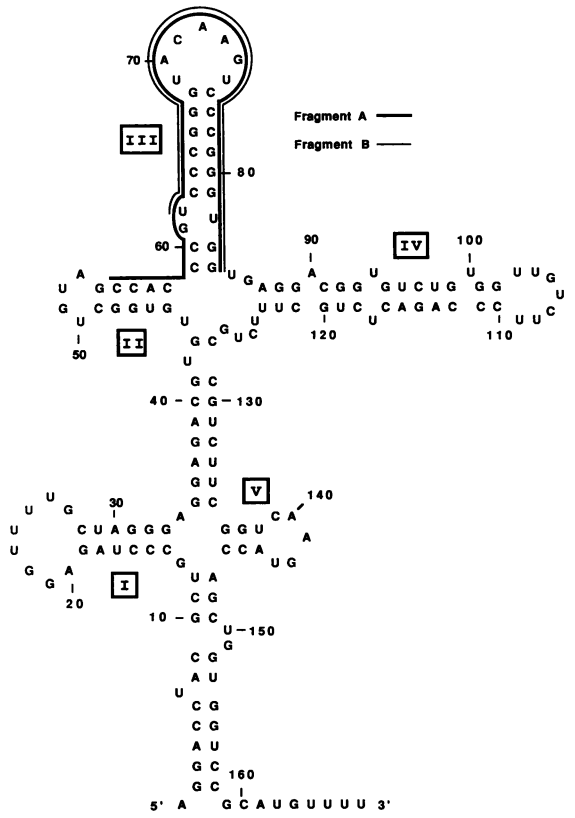

FIG. 4. EBER 1 secondary structure. The structure shown was previously determined experimentally (14). Boxed roman numerals indicate helices 1 through 5. The EBER 1 fragments identified in RNase protection experiments (A and B in Fig. 3) are shown on the EBER 1 structure as lines parallel to the corresponding sequence.

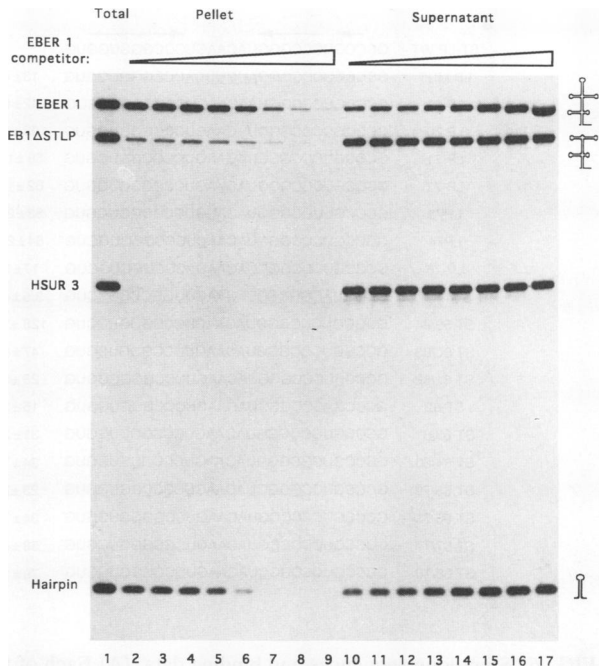

FIG. 5. EAP binding to EBER 1 mutants. A total of 0.8 fmol (each) radiolabelled EBER 1, EB1ΔSTLP, HSUR 3, and hairpin (stem-loop 3) was added to BJAB whole-cell sonicate in the presence of various concentrations of unlabelled EBER 1 competitor. After a short incubation, EAP-associated RNAs were immunoprecipitated with anti-EAP serum and fractionated on an 8% sequencing gel. Lanes: 1, total input RNA; 2 to 9, immunoprecipitated RNAs; 10 to 17, RNAs from the corresponding supernatants. A total of 0, 0.18, 0.57, 1.8, 5.7, 18, 57, or 180 pmol of cold EBER 1 was added to the samples shown in lanes 2 to 9 (and lanes 10 to 17), respectively.

interactions since, unlike bands A and B, they are also seen in some control experiments with preimmune serum (not shown). Enzymatic RNA sequencing (data not shown) revealed that the most prominent fragment, fragment A, corresponds to C55-G84(83) of EBER 1. This sequence is located in the third stem-loop of EBER 1 (Fig. 4). The second fragment, fragment B, is a smaller piece of this same hairpin structure [U62-G84(83)].

Although these analyses strongly suggest a specific interaction between EAP and stem-loop 3, they do not show that this region of EBER 1 is necessary and sufficient for EAP binding. To address this question, we produced mutants of EBER 1 which lack this stem-loop (EB1ΔSTLP), as well as constructs which retain only stem-loop 3. The efficiency with which EAP binds these in vitro-transcribed RNAs was determined by adding them to extracts of uninfected cells and then assessing their immunoprecipitabilities with anti-EAP antibodies. In vitro-transcribed EBER 1 served as a positive control, while HSUR 3 (a viral small RNA which is not known to bind EAP [21, 26]) provided a negative control. Precipitations were performed after a brief incubation in the presence of increasing concentrations of an unlabelled specific competitor (EBER 1). Unpublished control experiments indicate that anti-EAP antibodies do not recognize the naked EBER 1 molecule.

Figure 5 shows that stem-loop 3 (labelled hairpin) binds EAP very well (65 versus 78% precipitation for hairpin and EBER 1, respectively; quantitation of Fig. 5, lane 2). Moreover, stem-loop 3 is specifically competed at a competitor concentration only slightly lower than the concentration at which EBER 1 itself is competed (lane 6 versus lane 7). Lane 6 probably represents the point at which EAP is no longer in excess over EBER 1. Interestingly, EB1ΔSTLP (lacking stem-loop 3) also shows significant immunoprecipitation (21%; lane 2) which, unlike HSUR 3 precipitation, which is at a constant low level (3.5%), is specifically competed by unlabelled EBER 1. These data suggest that although stem-loop 3 is largely responsible for EAP's binding to EBER 1, there may be an additional binding site(s) elsewhere on EBER 1.

EAP recognizes both single-stranded and double-stranded regions of stem-loop 3. To determine which nucleotides in stem-loop 3 are required for EAP binding, we tested a large number of stem-loop 3 mutants for their abilities to bind EAP. These RNAs were transcribed from synthetic deoxyoligonucleotides encoding the T7 RNA polymerase promoter followed by the desired sequence. The mutants (Fig. 6) fall into two general categories: LP mutants are transversions of each of the nucleotides in the loop region (nucleotides 69 to 75), and ST mutants alter the stem region such that potential base-pairing partners are exchanged (e.g., G68 was changed to C, and its partner, C76, was made a G; an exception is the bulged nucleotide U62, which was simply changed to an A).

Each mutant RNA was tested as in Fig. 5 for its ability to bind EAP (Fig. 7). Again we chose to examine cellular EAP rather than the fusion protein, which may exhibit subtle

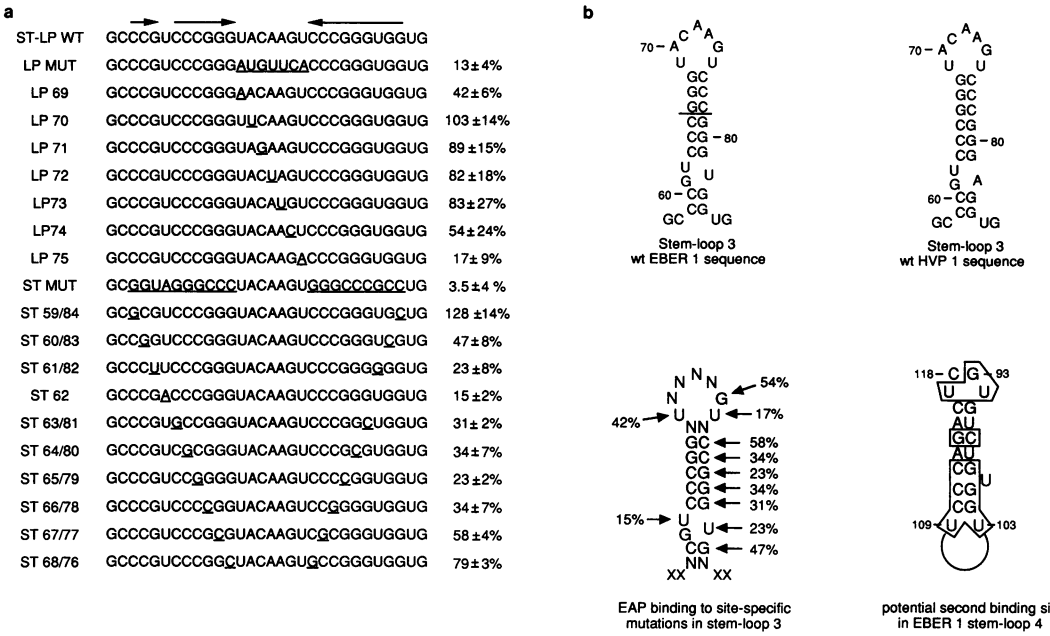

FIG. 6. Stem-loop sequences and binding data. (A) Each of the mutant stem-loops used in Fig. 7 is shown as a linear sequence with the base-paired stem designated by arrows. The mutated nucleotide(s) is underlined. The binding ability of each hairpin is shown on the right, expressed as a percentage of wild-type binding (i.e., ST-LP WT is 100% by definition). The error shown indicates a standard deviation for the LP mutants ($n = 3$) or the range for the stem mutant RNAs ($n = 2$). (B) The upper-left and upper-right hairpins represent the wild-type stem-loop 3 sequences of EBER 1 and HVP 1, respectively. The bar placed within the EBER 1 stem-loop 3 structure indicates an axis of symmetry. The bottom-left structure shows those nucleotides or base pairs in stem-loop 3 which, when changed to a given sequence (see panel a), decrease EAP binding to the level specified. N indicates a nucleotide or a base pair that can be altered to at least one other sequence without causing a greater-than-twofold reduction in EAP binding. X indicates nucleotides present in all mutants (see panel a) but untested for their role in EAP binding. The bottom-right structure shows a region of EBER 1 stem-loop 4 (nucleotides 93 to 103 and 109 to 118) which may be responsible for EB1ΔSTLP's ability to bind EAP. Boxed regions represent matches to the stem-loop 3 binding site.

differences in RNA binding. EBER 1 and HSUR 3 acted as positive and negative controls, respectively. Relative quantitation of the binding data (Fig. 6) shows that many of the single-stranded (loop) nucleotides are not required for efficient binding; however, mutating the two uridines that abut the stem (U62 and U75) does strongly decrease immunoprecipitability. Conversely, almost all mutations in the stem (Fig. 7b) except those in the base pairs close to the loop decrease binding by at least twofold. Note that while mutations such as these establish that a particular nucleotide or base pair is being recognized in a sequence-specific fashion, they do not show that the nucleotide(s) being analyzed is the only one(s) which is functional. Likewise, we do not know whether those nucleotides whose identity appears not to be important (N in Fig. 6b) can, in fact, be any nucleotide, since we have examined only certain changes.

DISCUSSION

The EBERs are by far the most abundant viral transcripts expressed during latent infection of human B cells by EBV. Nonetheless, the functions of both the EBERs and the homologous small RNAs encoded by HVP remain obscure. We have shown that EAP, an abundant, highly conserved

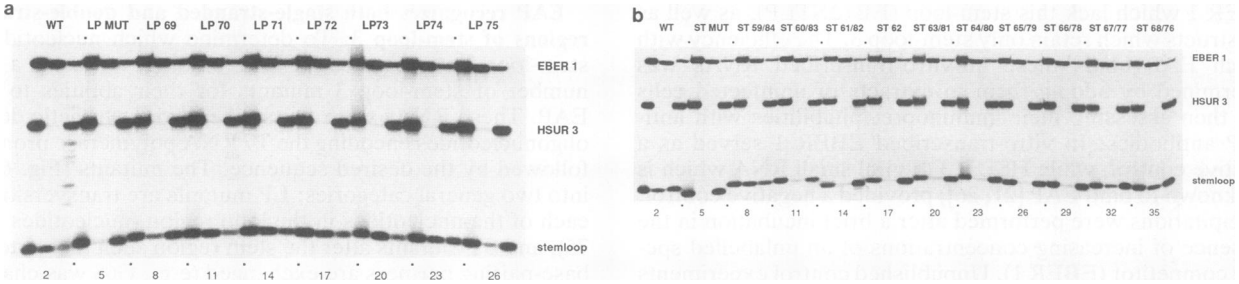

FIG. 7. Testing stem-loop 3 mutants for their abilities to bind EAP. Each of the stem-loop 3 mutants shown in Fig. 6a was assayed for its ability to bind EAP in a BJAB cell sonicate. EBER 1 and HSUR 3 were added as internal controls. After a 10- to 15-min reconstitution at 25°C, EAP-associated RNAs were selected by immunoprecipitation with anti-EAP serum and run on an 8% sequencing gel. For each stem-loop variant examined, equivalent samples of total added RNA, EAP-bound RNA, and unbound RNA are shown (lanes 1 to 3, 4 to 6, and 7 to 9, etc.).

cellular protein which binds EBER 1 and HVP 1, specifically recognizes a stem-loop structure that is conserved between these two RNAs. Using antibodies generated against EAP, we have demonstrated that binding is sensitive to mutations in both the single-stranded loop and the base-paired stem of this structure.

The EAP-binding site. The binding of EAP to EBER 1 is a direct association that can occur in the absence of any posttranslational modifications or other viral or host polypeptides. This conclusion is based on the observation that a bacterially expressed GST-EAP fusion protein specifically binds EBER 1 (Fig. 2a), recognizing the same stem-loop region as the native human protein (data not shown). Reconstitution experiments with EBER 1 mutants (Fig. 5) strongly argue that stem-loop 3, first identified by RNase protection experiments (Fig. 3), can bind EAP independently of the rest of the EBER 1 molecule. The fact that an interaction between EAP and EBER 2 is not detected by the immunoprecipitation and RNase protection experiments described here suggests that the EBER 2 binding previously observed (32) may have been the result of contamination by EBER 1 or an EBER 1 breakdown product. This interpretation is consistent with structure-mapping analyses which indicate that EBER 1, but not EBER 2, is highly protected from nuclease digestion and chemical modification in whole-cell extracts (14).

Unexpectedly, the EBER 1 mutant lacking stem-loop 3 (EB1ΔSTLP) was also precipitable with anti-EAP antibodies, albeit much less efficiently than wild-type EBER 1 (Fig. 5). It may be that we have subdivided the EAP-binding site into two separate domains, each of which retains some ability to bind EAP. It is more likely, however, that EBER 1 has the capacity to bind more than one molecule of EAP. Nucleotides 93 to 103 and 109 to 117 of EBER 1 also match the EAP-binding site quite well (Fig. 6b). Since this potential second binding site contains most of the recognition sequence in the proper structural context, it may be responsible for the reduced level of EAP binding seen for EB1ΔSTLP. In confirmation of this hypothesis, we have found that 3′-terminal EBER 1 fragments starting at G92, G93, U94, or G95, but not those at N>95, are able to bind to the GST-EAP fusion protein (data not shown). Interestingly, the region of EBER 1 that corresponds to the potential second EAP-binding site is not conserved in HVP 1, which may explain in part why HVP 1 is immunoprecipitated less efficiently than EBER 1 by anti-EAP antibodies. Although EBER 1 stem-loop 3 is precipitable to a greater extent than EB1ΔSTLP, its binding is competed more easily (Fig. 5; compare lanes 2 and 6). There are several possible explanations; the majority of the EB1ΔSTLP RNA (but not EBER 1 or the hairpin RNA) may assume a conformation or be bound by some other protein that prevents EAP binding or, alternatively, a less abundant protein which binds stem-loop 3, but not EBER 1 or EB1ΔSTLP, could more easily compete for stem-loop 3 binding when EAP is limiting.

It is tantalizing that the EAP-binding site is largely palindromic (Fig. 6b). Nucleotides G61-U69 and G74-U82 represent a perfectly palindromic region both in sequence and secondary structure if one assumes that nucleotides G61 and U82 are not base paired, as was previously concluded by Glickman et al. (14). The analogous hairpin in HVP 1 does not maintain this base pair (Fig. 6b). The existence of a palindromic binding site suggests that two EAP molecules may associate with the stem-loop 3 structure. Yet, mutations in "equivalent" base pairs did not always give similar results: for example, a mutation at 63/81 strongly decreases binding, whereas a mutation at 68/76 has little or no effect (Fig. 7b; compare lanes 20 and 35). Moreover, many mutations within the palindrome decrease binding by more than 50% (Fig. 6). This observation is incompatible with the existence of two independent binding sites for EAP, but it allows for the possibility of cooperative binding. The coat protein of the *E. coli* phage R17 binds a specific RNA hairpin as a dimer and associates with multiple sites on R17 genomic RNA cooperatively during encapsidation (33).

EAP as an RNA hairpin-binding protein. The primary structure of EAP does not contain any of the established RNA-binding motifs that have been recently identified. The most thoroughly studied of these is the RNA recognition motif (1; for reviews, see references 3, 17, and 24) which appears in many single-strand-specific RNA-binding proteins, especially those that are structural components of small ribonucleoproteins and heterogeneous nuclear ribonucleoproteins. These include poly(A)-binding protein (30), the La protein (6), the polypyrimidine tract-binding protein (5), a number of the heterogeneous nuclear ribonucleoproteins (1), the U1 70K and A proteins (27, 31), U2-B″ (27), and a group of splicing factors which appear to bind pre-mRNA (e.g., *sex-lethal*, reviewed in reference 11).

EAP, on the other hand, fits better into a group of small, basic RNA-binding proteins, some of which contain the motif discussed by Lazinski et al. (20). Although it does not contain this motif, EAP does contain a number of clustered basic amino acid stretches (32). Also, EAP's requirement for a specific combination of bulged and double-stranded sequences in its binding site is shared by other members of this group, such as the human immunodeficiency virus Tat protein (7; also see references therein). Several ribosomal proteins also fit into this category (20); the few binding sites which have been mapped appear to consist of complicated rRNA secondary structures, as opposed to simple single-stranded regions (reviewed in reference 9).

Roles for the EBER-EAP interaction. The fact that EBER 1 may have two binding sites for EAP, together with the EBERs' extremely high abundance in cells latently infected with EBV, suggests that EBER 1 may be functioning to sequester a significant fraction of the cellular EAP molecules. Unpublished experiments show that the EBERs bind at least 30% of the EAP in an EBV-infected cell. It is therefore extremely important to determine the cellular target of EAP. The observation that anti-EAP immunoprecipitates do not contain high levels of any cellular RNA may indicate either that the epitope recognized by our antibodies is inaccessible in native particles or that the interaction between EAP and its cellular target RNA is unable to withstand the conditions used in our experiments. The latter seems unlikely, since >90% of EBER 1 can be bound to the GST-EAP fusion protein, even in the presence of 1 M urea (data not shown). An even less probable hypothesis is that EAP does not bind RNA at all in uninfected cells.

Anti-EAP immunoprecipitation patterns from cells labeled with ^{32}P in vivo display a low level of rRNA (≈5% of the total). Comparison of the profile from uninfected cells (Fig. 2b, lane 7) with a darker exposure of the preimmune control (lane 4) confirms a selective but minor enrichment of the 5S and 5.8S small rRNAs. Their immunoprecipitation may be due to an interaction of EAP either with ribosomes or with mRNA in polysomes. However, given the abundance of rRNA and the fact that only a minor fraction of it can be immunoprecipitated with anti-EAP antibodies, it is difficult to determine whether this result is biologically meaningful. A role for EAP in translation would be consistent with EAP's

abundance ($\approx 10^7$ per cell) and ubiquitous expression; we have found EAP to be highly expressed in all tissue culture cell lines tested. It is interesting that the only small viral RNA of known function, VAI RNA of adenovirus, has been shown to act at the level of translation (23). Given the similarities between the VAs and the EBERs (4, 28), an association between EBER 1 and a protein that interacts with ribosomes is a tantalizing possibility.

ACKNOWLEDGMENTS

We thank D. Wassarman, K. Soldatkin, S. Seiwert, S. Baserga, and V. Myer for helpful discussions, E. Sontheimer and K. Montzka Wassarman for help with RNA sequencing, and V. Myer for critical reading of the manuscript.

This work was supported by NIH grant CA 16038.

REFERENCES

1. **Adam, S. A., T. Nakagawa, M. S. Swanson, T. K. Woodruff, and G. Dreyfuss.** 1986. mRNA polyadenylate-binding protein: gene isolation and sequencing and identification of a ribonucleoprotein consensus sequence. Mol. Cell. Biol. **6**:2932–2943.
2. **Ausubel, F. M., R. Brent, R. E. Kingston, D. D. Moore, J. G. Seidman, J. A. Smith, and K. Struhl (ed.).** 1989. Current protocols in molecular biology. Wiley, New York.
3. **Bandziulis, R. J., M. S. Swanson, and G. Dreyfuss.** 1989. RNA-binding proteins as developmental regulators. Genes Dev. **3**:431–437.
4. **Bhat, R. A., and B. Thimmappaya.** 1985. Construction and analysis of additional adenovirus substitution mutants confirms the complementation of VAI RNA function by two small RNAs encoded by Epstein-Barr virus. J. Virol. **56**:750–756.
5. **Bothwell, A. L., D. W. Ballard, W. M. Philbrick, G. Lindwall, S. E. Maher, M. M. Bridgett, S. F. Jamison, and M. A. Garcia-Blanco.** 1991. Murine polypyrimidine tract binding protein. Purification, cloning, and mapping of the RNA binding site. J. Biol. Chem. **266**:24657–24663.
6. **Chambers, J. C., D. Kenan, B. J. Martin, and J. D. Keene.** 1988. Genomic structure and amino acid sequence domains of the human La autoantigen. J. Biol. Chem. **263**:18043–18051.
7. **Delling, U., L. S. Reid, R. W. Barnett, M. Y.-X. Ma, S. Climie, M. Sumner-Smith, and N. Sonenberg.** 1992. Conserved nucleotides in the TAR RNA stem of human immunodeficiency virus type 1 are critical for Tat binding and *trans* activation: model for TAR RNA tertiary structure. J. Virol. **66**:3018–3025.
8. **Dolecki, G. J., R. Lum, and T. Humphreys.** 1988. A gene expressed in the endoderm of the sea urchin embryo. DNA **7**:637–643.
9. **Draper, D. E.** 1989. How do proteins recognize specific RNA sites? New clues from autogenously regulated ribosomal proteins. Trends Biochem. Sci. **14**:335–338.
10. **England, T. E., A. G. Bruce, and O. C. Uhlenbeck.** 1980. Specific labelling of the 3′ termini of RNA with T4 RNA ligase. Methods Enzymol. **65**:65–74.
11. **Frankel, A. D., I. W. Mattaj, and D. C. Rio.** 1991. RNA-protein interactions. Cell **67**:1041–1046.
12. **Fregien, N., G. J. Dolecki, M. Mandel, and T. Humphreys.** 1983. Molecular cloning of five individual stage- and tissue-specific mRNA sequences from sea urchin pluteus embryos. Mol. Cell. Biol. **3**:1021–1031.
13. **Germino, J., J. G. Gray, H. Charbonneau, T. Vanaman, and D. Bastia.** 1983. Use of gene fusions and protein-protein interaction in the isolation of a biologically active regulatory protein: the replication initiator protein of plasmid R6K. Proc. Natl. Acad. Sci. USA **80**:6848–6852.
14. **Glickman, J. N., J. G. Howe, and J. A. Steitz.** 1988. Structural analyses of EBER 1 and EBER 2 ribonucleoprotein particles present in Epstein-Barr virus-infected cells. J. Virol. **62**:902–911.
15. **Howe, J. G., and M. D. Shu.** 1988. Isolation and characterization of the genes for two small RNAs of herpesvirus papio and their comparison with Epstein-Barr virus-encoded EBER RNAs. J. Virol. **62**:2790–2798.
16. **Howe, J. G., and M. D. Shu.** 1989. Epstein-Barr virus small RNA (EBER) genes: unique transcription units that combine RNA polymerase II and III promoter elements. Cell **57**:825–834.
17. **Kenan, D. J., C. C. Query, and J. D. Keene.** 1991. RNA recognition: towards identifying determinants of specificity. Trends Biochem. Sci. **16**:214–220.
18. **Kieff, E., and D. Liebowitz.** 1990. Epstein-Barr virus and its replication, p. 1889–1920. *In* B. N. Fields and D. M. Knipe (ed.), Virology. Raven Press, New York.
19. **Klein, G.** 1989. Viral latency and transformation: the strategy of Epstein-Barr virus. Cell **58**:5–8.
20. **Lazinski, D., E. Grzadzielska, and A. Das.** 1989. Sequence-specific recognition of RNA hairpins by bacteriophage antiterminators requires a conserved arginine-rich motif. Cell **59**:207–218.
21. **Lee, S. I., S. C. S. Murthy, J. J. Trimble, R. C. Desrosiers, and J. A. Steitz.** 1988. Four novel U RNAs are encoded by a herpesvirus. Cell **54**:599–607.
22. **Lerner, M. R., N. C. Andrews, G. Miller, and J. A. Steitz.** 1981. Two small RNAs encoded by Epstein-Barr virus and complexed with protein are precipitated by antibodies from patients with systemic lupus erythematosus. Proc. Natl. Acad. Sci. USA **78**:805–809.
23. **Mathews, M., and T. Shenk.** 1991. Adenovirus virus-associated RNA and translation control. J. Virol. **65**:5657–5662.
24. **Mattaj, I.** 1989. A binding consensus: RNA-protein interactions in splicing, snRNPs, and sex. Cell **57**:1–3.
25. **Miller, I. G.** 1990. Epstein-Barr virus: biology, pathology, and medical aspects, p. 1921–1958. *In* B. N. Fields and D. M. Knipe (ed.), Virology. Raven Press, New York.
26. **Myer, V., S. I. Lee, and J. A. Steitz.** 1992. Viral snRNPs bind a protein implicated in messenger RNA destabilization. Proc. Natl. Acad. Sci. USA **89**:1296–1300.
27. **Query, C. C., R. C. Bentley, and J. D. Keene.** 1989. A common RNA recognition motif identified within a defined U1 RNA binding domain of the 70K U1 snRNP protein. Cell **57**:89–101.
28. **Rosa, M. D., E. Gottlieb, M. R. Lerner, and J. A. Steitz.** 1981. Striking similarities are exhibited by two small Epstein-Barr virus-encoded ribonucleic acids and the adenovirus-associated ribonucleic acids VAI and VAII. Mol. Cell. Biol. **1**:785–796.
29. **Rüther, U., and B. Müller-Hill.** 1983. Easy identification of cDNA clones. EMBO J. **2**:1791–1794.
30. **Sachs, A. B., M. W. Bond, and R. D. Kornberg.** 1986. A single gene from yeast for both nuclear and cytoplasmic polyadenylate-binding protein: domain structure and expression. Cell **45**:827–835.
31. **Scherly, D., W. Boelens, N. A. Dathan, W. J. van Venrooij, and I. W. Mattaj.** 1990. Major determinants of the specificity of interaction between small nuclear ribonucleoproteins U1A and U2B″ and their cognate RNAs. Nature (London) **345**:502–506.
32. **Toczyski, D., and J. A. Steitz.** 1991. EAP, a highly conserved cellular protein associated with Epstein-Barr virus small RNAs (EBERs). EMBO J. **10**:459–466.
33. **Witherell, G. W., J. M. Gott, and O. C. Uhlenbeck.** 1991. Specific interaction between RNA phage coat proteins and RNA. Prog. Nucleic Acid Res. Mol. Biol. **40**:185–220.